Icarus xxx (xxxx) xxx

Contents lists available at ScienceDirect

Icarus

journal homepage: www.elsevier.com/locate/icarus

Research Paper

The sublimative evolution of (486958) Arrokoth

Jordan K. Steckloff [a,b,*], Carey M. Lisse [c], Taylor K. Safrit [d], Amanda S. Bosh [d], Wladimir Lyra [e], Gal Sarid [f]

[a] Planetary Science Institute, Tucson, AZ, United States of America
[b] University of Texas at Austin, Austin, TX, United States of America
[c] Johns Hopkins University, Applied Physics Laboratory, Laurel, MD, United States of America
[d] Massachusetts Institute of Technology, Cambridge, MA, United States of America
[e] New Mexico State University, Las Cruces, NM, United States of America
[f] SETI Institute, Mountain View, CA, United States of America

ARTICLE INFO

Keywords:
Kuiper Belt
Rotational dynamics
Ices

ABSTRACT

We consider the history of *New Horizons* target (486958) Arrokoth in the context of its sublimative evolution. Shortly after the Sun's protoplanetary disk (PPD) cleared, the newly intense sunlight sparked a sublimative period in Arrokoth's early history that lasted for ~10–100 Myr. Although this sublimation was too weak to significantly alter Arrokoth's spin state, it could drive mass transport around the surface significant enough to erase topographic features on length scales of ~10–100 m. This includes craters up to ~50–500 m in diameter, which suggests that the majority of Arrokoth's craters may not be primordial (dating from the merger of Arrokoth's lobes), but rather could date from after the end of this sublimative period. Thereafter, Arrokoth entered a Quiescent Period (which lasts to the present day), in which volatile production rates are at least 13 orders of magnitude less than the ~10^{24} molecules/s detection limit of the *New Horizons* spacecraft (Lisse et al. 2020). This is insufficient to drive either mass transport or sublimative torques. These results suggest that the observed surface of Arrokoth is not primordial, but rather dates from the Quiescent Period. By contrast, the inability of sublimative torques to meaningfully alter Arrokoth's rotation state suggests that its shape is indeed primordial, and its observed rotation is representative of its spin state after formation.

1. Introduction

(486958) Arrokoth is a cold classical Kuiper Belt Object (KBO), which is thought to have formed at 44.6 au from the Sun, where it has resided ever since (Stern et al., 2019). This stability is unique amongst all objects previously visited by spacecraft, which are thought to have moved and migrated due to instabilities amongst the giant planets and disk-planet interaction after formation. Thus, Arrokoth provides an opportunity to study how thermally driven processes could have evolved this object over the age of the Solar System, from formation in the Sun's protoplanetary disk (PPD) to the present. Because Arrokoth is rich in ices (Grundy et al., 2020; Lisse et al., 2020), early sublimative processes could have dramatically altered its surface features and appearance, and even its behavior if vigorous enough, e.g. affecting the spin state of the body via the effects of sublimative torques. Indeed, such processes could be quite important in the evolution of Arrokoth, which (i) is thought to have formed from a gentle merger of two separate objects that bled off significant orbital and rotational angular momentum (Hirabayashi et al., 2020; McKinnon et al., 2020) and (ii) shows sufficient crater counts to date its surfaces to the earliest part of the Solar System's history (Spencer et al., 2020). Here we explore how sublimative activity may have affected Arrokoth over its history.

2. Periods of Arrokoth's history

Arrokoth formed in extremely cold conditions in the Sun's protoplanetary disk (PPD), sufficient for CO (Krijt et al., 2018) and other hypervolatile species (such as N_2, and CH_4) to condense into solids. Later, the Sun's T Tauri winds and gas accretion cleared out the protoplanetary disk (PPD); Arrokoth's surface was newly exposed to solar heating. At this point, the surface of Arrokoth was likely pristine, with hypervolatile CO, N_2, and CH_4 present (Lisse et al., 2020). The sublimation rate of these ices would have been very high, representing a maximum sublimative flux from the surface. However, as these volatiles

* Corresponding author.
E-mail address: jsteckloff@psi.edu (J.K. Steckloff).

https://doi.org/10.1016/j.icarus.2020.113998
Received 17 October 2019; Received in revised form 17 July 2020; Accepted 22 July 2020
Available online 3 August 2020
0019-1035/© 2020 Published by Elsevier Inc.

Please cite this article as: Jordan K. Steckloff, *Icarus*, https://doi.org/10.1016/j.icarus.2020.113998

sublimated away and depleted the body, Arrokoth would eventually cease to vigorously outgas, and would enter a steady state sublimative regime that exists to the present day. For this reason, we must separately consider these two periods: the "Sublimative Period" (shortly after the clearing of the Sun's PPD), and the "Quiescent Period" (began once Arrokoth reached a thermodynamic steady state).

2.1. Arrokoth's Sublimative Period

We can estimate the duration of the Sublimative Period by computing how long the post PPD thermal wave would require to reach the center of the body (and hence the time after which the primitive thermal structure is lost). Although there has been some advancement in past work regarding the thermophysical evolution of KBO surfaces and interiors, there are still many basic open questions, large parameter uncertainties, and a lack of constraints for ranges of physical parameters. Specific to our modeling work in this paper are the important issues of object size, density, and assumed composition. In many respects, while Arrokoth is clearly a member of the cold-classical KBO dynamical grouping, its size and probable density of ~300–500 kg/m^3 (Hirabayashi et al., 2020; McKinnon et al., 2020) is physically most akin to a large comet nucleus (e.g., Richardson et al., 2007; Thomas et al., 2013a, 2013b; Pätzold et al., 2016, Kokotanekova et al., 2017; Preusker et al., 2017). The two distinct lobes may even be considered as proxies for two small comet nuclei (roughly 7.5 and 10 km in radius), as their internal thermal evolution has probably initiated and progressed with minimal cross-influence in the deep interior, similarly to other small icy bodies (e.g., Davidsson et al., 2016; McKinnon et al., 2020).

In contrast, previous work dealing with the thermophysical evolution of KBOs has largely focused on significantly larger objects with higher densities than Arrokoth (e.g., De Sanctis et al., 2001, 2007; Merk and Prialnik, 2003; Choi et al., 2002; Prialnik et al., 2008; Sarid and Prialnik, 2009; Desch et al., 2009; Guilbert-Lepoutre et al., 2011). Although some of the studied examples are only an order of magnitude greater in volume than Arrokoth (e.g., De Sanctis et al., 2001; Prialnik et al., 2008; Sarid and Prialnik, 2009), these examples are nevertheless much too large to be applicable to Arrokoth; especially in the effects of radiogenic heating, for which the amplitude of heating depends directly on size. The net thermal energy deposition results form a balance between heat loss through the surface and heat production within the interior. Thus, the smaller the object's radius, the lower the maximum temperature it can attain. Indeed, while sophisticated models exhibit the dependence on size, density, composition, and radionuclide abundance, many studies of icy body radiogenic heating have shown that the amplitude of this effect is negligible for water ice rich bodies (mostly in mixed crystalline and amorphous form) with radii smaller than ~10–15 km (e.g., Prialnik and Podolak, 1995; De Sanctis et al., 2001; Choi et al., 2002; Prialnik et al., 2008; Sarid and Prialnik, 2009).

To estimate the characteristic timescale of the Sublimative Period, we rearrange the thermal skin depth equation, which measures the distance below the surface at which the amplitude of a surface thermal wave decreases by $1/e$:

$$d_{skin} = \sqrt{\mathscr{K} t} \tag{1}$$

$$t = \frac{d_{skin}^2}{\mathscr{K}} \tag{2}$$

where d_{skin} is the thermal skin depth, $\mathscr{K}$ is the thermal diffusivity, and t is the elapsed time. Thermal diffusivity measures the ease with which a heat wave diffuses into a surface, and is related to the thermal conductivity (k), specific heat capacity (c_p), and density (ρ) by

$$\mathscr{K} = \frac{k}{\rho c_p}. \tag{3}$$

For Arrokoth, we use its most plausible density range of ~300–500 kg/m^3 (Hirabayashi et al., 2020; McKinnon et al., 2020), and the specific heat capacities for volatile ices, which are on the order of ~2000 J/kg K (the specific heat capacity of water ice). The thermal conductivity of porous cometary material is on the order of $\sim 10^{-2}$–10^{-1} W/K m (Gundlach and Blum, 2012), resulting in a thermal diffusivity of $\sim 10^{-8}$–10^{-7} m^2/s.

Alternatively, thermal inertia (I), which measures a surface's resistance to changing its temperature in response to a changing thermal environment, is related to thermal conductivity, specific heat capacity, and density by

$$I = \sqrt{k \rho c_p} \tag{4}$$

thus

$$\mathscr{K} = \frac{I^2}{\rho^2 {c_p}^2} \tag{5}$$

The thermal diffusivity of the surface of Comet 67P/Churyumov-Gerasimenko is 80_{-40}^{+80} JK^{-1}m^{-2}s$^{-0.5}$ (Marshall et al., 2018) with a density of 537.8 ± 0.7 kg/m^3 (Preusker et al., 2017), with a specific heat capacity modeled to be around ~350 (Grundy et al., 2020) to ~1000 J kg^{-1} K^{-1} (Hu et al., 2017), 2×10^{-8} (6×10^{-9} - 9×10^{-8}) m^2/s, which is consistent with this range of thermal diffusivities.

These values are smaller than the thermal diffusivities of typical geological materials (~10^{-6} $\frac{m^2}{s}$; Drury, 1987) due to the low densities and high porosities of small icy bodies.[1] From this thermal diffusivity range, the thermal wave of the Sun would reach the centers of Arrokoth's lobes ~10–100 Myr after the dispersal of the PPD. This calculation assumes that the clearing of the PPD occurred instantaneously. While this is not strictly true (and indeed was likely to have occurred over a timescale of up to a few million years; Williams and Cieza, 2011), this is sufficiently short to not affect these order of magnitude estimates of Arrokoth's Sublimative Period duration.

It is important to remember that the two lobes of Arrokoth have a smaller effective radius than their long-axis radius. When considering a more realistic representation of the "flat ellipsoid" shape of Arrokoth's lobes (McKinnon et al., 2020), we can expect the internal thermal evolution to be less secular and advance in a more episodic pattern and at a faster rate at different locations within the body, especially if internal inhomogeneities are present (e.g. Rosenberg and Prialnik, 2010; Guilbert-Lepoutre et al., 2016). Hence, these thermal evolution timescales are likely an estimate for the upper limit of the volatile-active, sublimative period, in Arrokoth's evolution.

During the Sublimative Period, some volatiles outgassed vigorously, while others maintained extremely low production rates. To compute the sublimative flux of these volatiles, we use the model of Steckloff et al. (2015), which solves the energy balance equation at the surface of the body, accounting for solar heating, and both radiative and sublimative cooling. This model uses first principles (Clausius-Clapyron relation, Langmuir-Knudsen equation of sublimation rates [Langmuir, 1913], conservation of energy, and conservation of momentum) to solve for the sublimative molecular flux and sublimative back reaction pressure exerted on the surface. Using this model, we can constrain the sublimative flux of CO from the surface of Arrokoth to up to ~4×10^{29} molecules per second. N_2 ice would behave similarly to CO (Lisse et al., 2020). Due to their much higher enthalpy of sublimation, sublimative cooling from other common icy volatiles such as H_2O and CO_2 are at least eighteen orders of magnitude lower at 44.6 AU, Arrokoth's distance from the Sun (see Fig. 1), and are therefore insignificant in the Sublimative Period. Thus, Arrokoth would effectively cease to outgas

[1] Grundy et al. (2020) assumed thermal properties that recreate ground-based observations of KBOs, but result in thermal diffusivity values 3–4 orders of magnitude small still, which would result in the Sublimative Period lasting for ~100 Gyr.

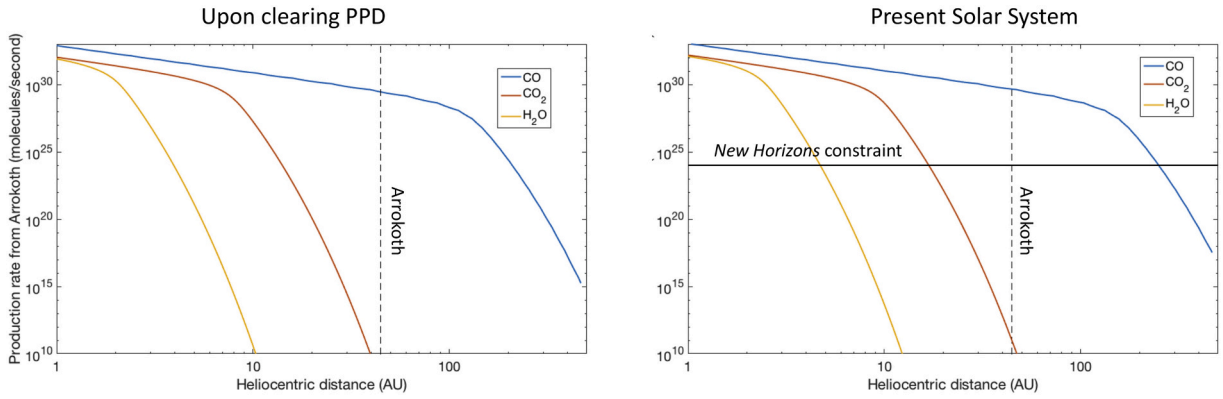

Fig. 1. The sublimative flux from a pristine Arrokoth-like object across the Solar System.(left) early Solar System; solar luminosity 70% present value (Sagan and Mullen, 1972) and (right) present Solar System. In both cases, at 44.6 au from the Sun, hypervolatiles such as CO would sublimate readily from the surface of Arrokoth. However, such volatiles would rapidly recede below its surface. Other common volatiles have extremely low sublimation rates from MU_{69} due to the extreme cold.

vigorously once depleted of CO and other minor supervolatiles.

2.2. Arrokoth's Quiescent Period

Once the thermal wave and supervolatile sublimation fronts reach Arrokoth's center, the supervolatiles will be depleted, ending Arrokoth's Sublimative Period. More refractory volatiles (e.g., CO_2, H_2O) would still be present within Arrokoth, however temperatures would be much too low to allow these volatiles to sublimate vigorously. Instead, volatiles will slowly be released from the volatile sublimation fronts, diffuse to the surface, and ultimately leave the body. The rate of volatile loss (and thus rate of sublimation front recession) would depend on the relative volatility of the species. For Example, CO_2's high volatility would cause this species to recede faster into the surface than H_2O. Eventually, these differences would be expected to produce a mature equilibrium subsurface structure on Arrokoth, similar to the expected subsurface structures of comets (Prialnik et al., 2004). Although these volatile fronts would continue to recede into Arrokoth, their extremely low outgassing rates (Fig. 1) suggests that this structure has changed little since formation (volatile fronts moved on the order of centimeters over the age of the solar system). Ultimately, the state observed by the *New Horizons* spacecraft is likely representative of the sublimative state and structure of Arrokoth at the dawn of the Quiescent Period, regardless of whether such unobservable layers exist.

3. Sublimative spin-state evolution

Sublimative outgassing of volatiles can produce torques that change an object's rotation state. Since Arrokoth is thought to have formed from the accretion of two lobes to form the bilobate shape observed by the *New Horizons* spacecraft, sublimative torques may have played a role in spinning down the lobes to facilitate merger (McKinnon et al., 2020) or spinning up the object to separate the lobes (Hirabayashi et al., 2016, 2020). However, the effects of sublimation early in Arrokoth's history (e.g., immediately after the clearing of the PPD) are much stronger than later in Arrokoth's history, due to supervolatiles being readily available near its surface. This requires that we explore these two regimes separately. Here we explore the limits and effects of such sublimative torques on the rotation state of Arrokoth.

To compute how such outgassing may change the rotation rate of Arrokoth, we use the SYORP sublimative torque model (Steckloff and Jacobson, 2016; Steckloff and Samarasinha, 2018), which repurposes the mathematical machinery of the YORP effect (taking advantage of the similarities in the behavior of radiative and sublimative processes). From this model, the maximum sublimative angular acceleration of Arrokoth is

$$\left|\frac{d\omega}{dt}\right| = \frac{3P_S C_S}{4\pi\rho R^2} \tag{6}$$

$$= \frac{3\Phi_{sub} m v_{thermal} C_S}{4\pi\rho R^2} \tag{7}$$

where P_S is the dynamic sublimation pressure exerted by the escaping gases on the surface, C_S is an empirical factor analogous to YORP coefficients, ρ is the bulk density of Arrokoth; R is the mean radius of Arrokoth, approximately 8.5 km (Stern et al., 2019), Φ_{sub} is the sublimative gas flux from the surface, m is the molecular mass of the volatile, and $v_{thermal}$ is the mean molecular thermal velocity of the molecule. This model assumes that the object has a very low albedo (consistent with the 6.3% bond albedo of Arrokoth [Hofgartner et al., 2020]), and is composed entirely of a single volatile ice (for example, CO). This model also assumes that the multiple different chemical species composing Arrokoth do not interact with one another. Such interactions can change molecular binding energies, and thus latent heats of sublimation. However, such effects are poorly understood, and beyond the current state of the art of comet science. Note that this equation only provides the magnitude of the angular acceleration, and that sublimative torques could spin the object up or down.

Like the YORP coefficients (Scheeres, 2007; Rozitis and Green, 2013), the SYORP coefficient C_S parameterizes how a body's spin pole obliquity and irregular shape leads to net torques (Steckloff and Jacobson, 2016). Unlike radiative processes in which the entire surface emits photons, much of the surfaces of icy bodies are sublimatively inactive. Thus, the SYORP coefficient C_S also accounts for the effects of volatile distribution on sublimative torques (Steckloff and Samarasinha, 2018). Additionally, SYORP coefficients must account for the collisional nature of gas molecules near the surfaces of icy bodies, which will cause gas molecules to spread out and collide with the surface, weakening the sublimative generation of torques. Pristine icy objects may have SYORP coefficients on the order of ~0.0001–0.001 (Steckloff and Jacobson, 2016), which is an order of magnitude lower than the typical range for YORP coefficients (Scheeres, 2007; Rozitis and Green, 2013). However, evolved objects with only partially sublimatively active surfaces likely have SYORP coefficients that are lower than this range.

To more accurately model sublimative torques, we use observed rotation state changes in short-period comets to compute the SYORP coefficients for these "real", evolved objects. We rearrange Eq. (6) to solve for C_S from observed rotation state changes and nucleus material properties. In cases where the bulk density of the nucleus is not known, we assume a typical range of comet bulk densities of 300–700 kg/m^3 (Steckloff and Samarasinha, 2018). We compute the SYORP coefficients

for comets 2P/Encke, 9P/Tempel 1, 10P/Tempel 2, 19P/Borrelly, 67P/Churyumov-Gerasimenko, and 103P/Hartley 2, and find that they span a relatively narrow range of values, 1.22×10^{-5} - 8.43×10^{-5} (see Table 1).

We use these values to compute the effects of CO sublimative torques on Arrokoth shortly after formation (see Fig. 2), with the timescale of Arrokoth's changing rotation period depending on bulk density and efficiency of the sublimative torques (i.e., the SYORP coefficient C_S). We assume a bulk density for Arrokoth of between 300 and 500 kg/m^3 (Hirabayashi et al., 2020; consistent with McKinnon et al., 2020). The higher end of this plausible density range (500 kg/m^3; Hirabayashi et al., 2020; McKinnon et al., 2020) is typical of Jupiter Family Comets such as 67P/Churyumov-Gerasimenko (Pätzold et al., 2016) or (D/1993 F2) Shoemaker-Levy 9 (Asphaug and Benz, 1996). At this density, Arrokoth's lobes would separate at a spin period of 12.5 h (Hirabayashi et al., 2020), and sublimative torques would require ~0.1–10 Myr to spin down Arrokoth to its present 15.92 h spin period (assuming its maximum outgassing rate). However, such an outgassing rate would deplete Arrokoth of CO in only ~10,000 years. As a result, sublimative torques would have changed Arrokoth's rotation period by only as many as a few minutes to tens of minutes (depending on density and SYORP coefficient).

Although these timescales imagine a maximally outgassing Arrokoth, in reality such volatile loss rates would slow down as the sublimation front receded below the surface, allowing outgassing to last until the solar thermal wave reaches Arrokoth's center (the entire length of the sublimative period). Nevertheless, our modeling effort depends solely on the total volatile flux; the outgassing rate and duration are irrelevant over secular timescales so long as the total volatile flux is the same.

Arrokoth's shape is minimally stable at the lower end of its range of plausible densities of ~300–500 kg/m^3 (Hirabayashi et al., 2020; McKinnon et al., 2020), a density consistent with the density of comet 103P/Hartley 2 (Thomas et al., 2013a, 2013b; Richardson and Bowling, 2014). At such densities, Arrokoth's lobes separate at spin periods just below its present-day spin period; and sublimative torques could have caused the lobes to separate. However, at densities of even a few ~10's of kg/m^3 above this lower limit, sublimative torques would be insufficient to change Arrokoth's spin state sufficiently to cause its lobes to separate. Ultimately, sublimative torques are unlikely to have a significant effect on Arrokoth's spin state during the Sublimative Period, changing its spin period by a few minutes at most, before vigorous sublimation ceases.

Outgassing during Arrokoth's Quiescent Period similarly had a negligible effect on Arrokoth's spin state. We rearrange Eq. (7) to solve for the flux required to spin the nucleus up/down

$$\Phi_{sub} = \frac{4\pi\rho R^2 \Delta\omega}{3 m v_{thermal} C_S \Delta t} \tag{8}$$

where Δt is the duration of volatile sublimation (here 4.5 billion years) and $\Delta\omega$ is the change in angular speed, which we set to 10^{-6} to represent spin period changes on the order of a few minutes (comparable to the limit in the Sublimative Period). We use best-case parameters for Arrokoth to compute the lowest sublimative flux needed for this change: low density of 300 kg/m^3 (Hirabayashi et al., 2020; McKinnon et al., 2020), peak temperature of 58 K (Grundy et al., 2020) across the body, and high SYORP coefficient of 10^{-4}. Even with these best-case values, the average CO_2 flux from Arrokoth would need to be ~10^{17} molecules/s to change its spin period by a few minutes. However, the sublimative flux of CO_2, the most volatile major component of cometary ices following CO, would have a maximum flux from Arrokoth of only ~10^{11} molecules/s (Fig. 1). For lower SYORP values and higher bulk densities (which are more consistent with other typical Cold Classical Kuiper Belt Object density estimates of ~600–1400 kg/m^3; Vilenius et al., 2012; Grundy et al., 2012; Brown, 2013; Vilenius et al., 2014), the minimum flux increases to ~10^{18} molecules/s. Other, more volatile ices may contribute to this flux, but would have minor contributions. Thus, Arrokoth's spin state has changed negligibly since the end of the Sublimative Period.

Finally, we have thus far treated sublimative torques as monotonic increases or decreases in the rotation state of an object. However, sublimative torques are likely stochastic in direction, both spinning objects up and down (Statler, 2009; Cotto-Figueroa et al., 2015). With this consideration, the calculated changes in rotation rates may overestimate actual changes by an order of magnitude.

Considering that impacts have also changed Arrokoth's spin period by at most a few minutes (Hirabayashi et al., 2020), the present spin period is representative of Arrokoth's spin state upon the clearing of the Sun's protoplanetary disk. Similarly, sublimative torques are unlikely to have contributed to the initial formation of Arrokoth's contact binary shape. Arrokoth's shape is indicative of a gentle merger of the two lobes, suggesting a gentle process for eliminating orbital angular momentum from the system to cause the lobes to merge (McKinnon et al., 2020),

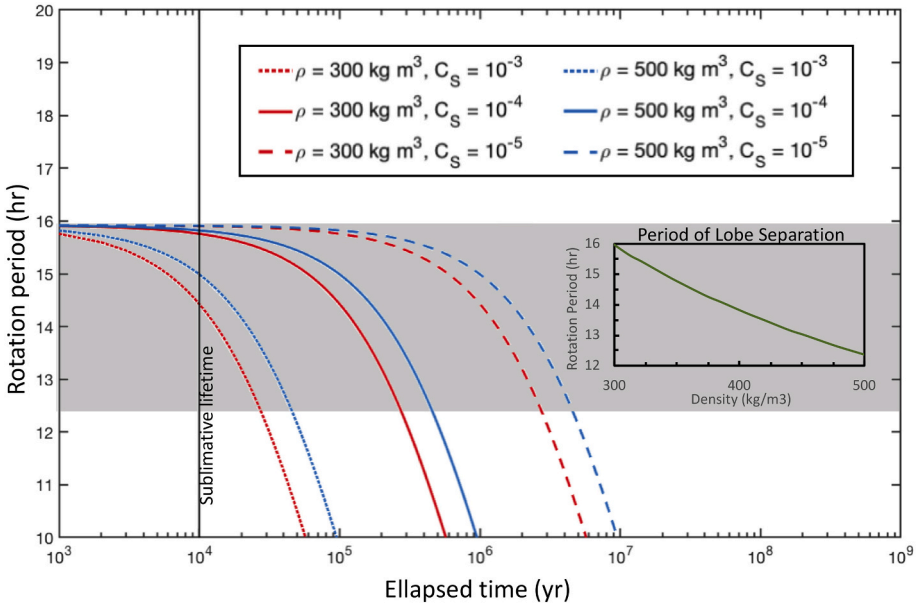

Fig. 2. Timescale of CO torques acting to change the rotation period of a pristine MU_{69}. Shortly after the PPD clears, CO sublimation may spin up MU_{69}. The spin period associated with lobe separation is highly density dependent, lying between 15.9 and 12.5 h for densities of 300–500 kg m^{-3} (Hirabayashi et al., 2020). If these torques remain constant, MU_{69} could have spun down from lobe separation/accretion over timescales of ~10^5 years (depending on density and sublimative torque strength), however Arrokoth could only sustain CO sublimation at this rate for only ~10,000 yr (its sublimative lifetime). Period of Lobe Separation replotted from Hirabayashi et al. (2020).

Table 1
Observed parameters of Jupiter-Family comets, used to compute SYORP coefficients. The SYORP coefficient C_S is a parameter that can be computed from observations and properties of comet nuclei. We find that the SYORP coefficients are 1–2 orders of magnitude smaller than those for pristine icy objects (Steckloff and Jacobson, 2016), and 2–3 orders of magnitude smaller than the analogous YORP coefficients for radiative torques (Scheeres, 2007; Rozitis and Green, 2013).

	Dominant Volatile species	Effective Radius (km)	Bulk Density (kg/m^3)	Rotation period (hr)	Observed Change in Rotation Period (min)	Computed SYORP Coefficient (C_S)
2P/Encke	H_2O	2.4[a,b]	300–700 (assumed)[c]	11[a,b]	4[a,b]	(3.7–8.6) × 10^{-5}
9P/Tempel 1	H_2O	2.83[a,b]	470_{-230}^{+780}[d,e]	41[a,b]	14[a,b]	$1.22_{-0.60}^{+2.03}$ × 10^{-5}
10P/Tempel 2	H_2O	6.0[a,b]	300–700 (assumed)[c]	9[a,b]	0.27[a,b]	(1.4–3.3) × 10^{-5}
19P/Borrelly	H_2O	2.52[b]	560 ± 270[f]	28[b]	40[b]	7.27(±3.50) × 10^{-5}
67P/Churyumov-Gerasimenko	H_2O	1.65[b]	533 ± 6[g]	12[b]	21[b]	8.43(±0.09) × 10^{-5}
103P/Hartley 2	CO_2	0.58[a,b]	300 ± 100[h]	18[a,b]	150[a,b]	1.70(±0.57) × 10^{-5}

[a] Samarasinha and Mueller (2013).
[b] Mueller and Samarasinha (2018).
[c] Reasonable range of cometary bulk densities (Steckloff and Samarasinha, 2018).
[d] Richardson et al. (2007).
[e] Thomas et al. (2013a).
[f] Farnham and Cochran (2002).
[g] Pätzold et al. (2016).
[h] Thomas et al. (2013b).

such as nebular drag (McKinnon et al., 2020; Lyra et al., 2020 submitted). Sublimative torques can only change the present angular momentum of the Arrokoth system by less than ~1% (assuming ideal conditions), and therefore contributed negligibly to the initial merger of Arrokoth's lobes. This further supports the notion that Arrokoth's shape is primordial (McKinnon et al., 2020).

4. Sublimative surface evolution

Volatile sublimation can drive topographic erosion (Britt et al., 2004; Steckloff and Samarasinha, 2018) and mass transport about the surface of an icy body (Lai et al., 2016). Rates of sublimation-driven erosion/deposition likely vary significantly within classes of icy bodies, and between different dynamical classes of bodies. Although a full calculation of these erosion/deposition rates on Arrokoth would require detailed simulations with many underconstrained variables. Nevertheless, if we assume that sublimation-driven evolution of Jupiter Family Comets is representative (when scaled) of icy bodies in the solar system, we can use existing studies of mass transport on JFCs to estimate the magnitude of mass transport/deposition on Arrokoth.

During the sublimative era, the surface vigorously sublimated CO and other supervolatiles. Using the sublimation model of Steckloff et al. (2015), we find that, even though CO is significantly more volatile than H_2O ice, the dynamic sublimation pressure driving and transporting dust about Arrokoth's surface is only ~0.5% as strong as H_2O's dynamic sublimation pressure on a typical JFC. Additionally, Arrokoth's large size gives it a surface escape speed and surface gravity on the order of 5 times greater than those of a typical JFC such as 67P/Churyumov-Gerasimenko (assuming comparable densities). Comparing these weak drag forces and higher gravity, the maximum loftable dust grain from Arrokoth would be ~0.1% the radius of the maximum loftable grain on 67P/Churyumov-Gerasimenko (on the order of hundreds of microns, rather than on the order of decimeters; Lai et al., 2016; Keller et al., 2017).

The grain size frequency distribution modeled in Lai et al. (2016) has a break in the power law differential size-frequency distribution at around a millimeter, with grains smaller than this following a power-law index of 2, and grains larger than this following a power-law index of 4 (a steeper drop-off with size (a power-law index of 3 indicates that mass is equally distributed amongst the grain sizes). Therefore, less mass is in the population of larger grains than in the population of smaller grains. Thus, if a similar grain-size distribution held true on Arrokoth, then the loss of these larger grains (which cannot be lofted on Arrokoth) would reduce the transported mass per unit area by less than 0.1% (relative to 67P). We adopt a 0.1% value as a conservative estimate.

Numerical models of thermally driven erosion and deposition are highly sensitive to model parameters. Nevertheless, numerous models explored the role of such processes on comet 67P/Churyumov-Gerasimenko, a Jupiter-Family Comet that was the target of the *Rosetta* mission, and found broad agreement in erosion/deposition rates. Global models found that the surface of 67P/Churyumov-Gerasimenko can erode on the order of ~4 m/year (Lai et al., 2016; Keller et al., 2017), and experience depositional growth on the order of ~0.5 m/yr (Lai et al., 2016) during an apparition. This is consistent with analysis of *Rosetta* images, which suggest erosion in many region of ~1 m and deposition of around ~20 cm (Hu et al. 2017). Other modeling efforts find that smooth terrains on 67P/Churyumov-Gerasimenko experience topographic evolution of ~1 m or less (Tang et al., 2019) or ~ 20 cm (Kossacki and Jasiak, 2019), although these terrains are themselves depositional, and can experience subsequent thermally driven topographic evolution (Birch et al., 2019). These results are consistent with the expectation that topographic changes occur more rapidly on steeper terrains than flatter terrains (Steckloff and Samarasinha, 2018).

Ultimately, these studies suggest that the erosion rate on comet 67P/Churyumov-Gerasimenko is on the order of ~0.2–4 m/year; thus, the scaled erosion rate on Arrokoth would be ~0.02–0.4 cm/yr. Arrokoth's higher escape speed and weaker sublimation pressures would result in negligible grain escape (unlike Jupiter family comets), resulting in a deposition rate that effectively matches the erosion rate. Thus, over the sublimative lifetime of Arrokoth (the time in which a block of CO the size of Arrokoth would completely disappear) of ~10,000 yr, the topography may erode/fill in, and ultimately change by as much as ~10–100 m during the sublimative period.

By comparison, sublimative forces during the quiescent period are effectively non-existent. The outgassing constraint observed by the *New Horizons* spacecraft would result in sublimation pressures more than 13 orders of magnitude smaller than those during the Sublimative Period. Dust transport under such conditions would undoubtedly be negligible, consistent with the lack of an observable dust coma during the *New Horizons* flyby.

These mass transport processes could profoundly alter the primordial surface of Arrokoth. Such erosion and deposition could effectively erase craters up to ~50–500 m across (assuming canonical depth/diameter ratio of 0.2). Indeed, most of the observed and suspected craters on Arrokoth fall in the upper end of this size range (Spencer et al., 2020). This suggests, rather provocatively, that the majority of the observed surface morphology and craters on Arrokoth may not date not from the

Sublimative Period, but rather from the Quiescent Period. In other words, although Arrokoth's shape is likely primordial, its surface may not be.

5. Conclusions

We consider the effects of sublimating volatiles on (486958) Arrokoth, and find that Arrokoth's sublimative history can be separated into two periods. An early Sublimative Period lasting ~10–100 Myr after the clearing of the Sun's protoplanetary disk (PPD), during which Arrokoth's supervolatile species such as CO sublimated vigorously. Such sublimation would cause significant erosion and dust transport about the surface, erasing surface features shallower than ~10–100 m. This includes craters up to ~50–500 m across, suggesting that the surface of Arrokoth we see today may not be primordial, but rather could date from after the Sublimative Period. Arrokoth's Sublimative Period was followed by a Quiescent Period, which continues to the present day. The Quiescent Period is marked by a lack of significant outgassing, with expected volatile production rates at least 13 orders of magnitude smaller than what *New Horizons* could detect. Sublimative torques have been insignificant throughout Arrokoth's history, suggesting that the present spin rate is representative of Arrokoth's primordial spin state, and that Arrokoth's shape, unlike its surface, is indeed primordial.

Declaration of Competing Interest

None.

Acknowledgments

The authors with to thank Seth Jacobson for productive conversations that helped explore the implications of this work. The authors also with to thank both anonymous reviewers, whose comments greatly improved the content, structure, organization, and ultimately, the conclusions and implications of this work. J.K.S. and G.S. acknowledge support from NASA award 80NSSC18K0497.

References

Asphaug, E., Benz, W., 1996. Size, density, and structure of comet shoemaker-levy 9 inferred from the physics of tidal breakup. Icarus 121, 225–248.

Birch, S.P.D., Hayes, A.G., Umurhan, O., Tang, M., Vincent, J.-B., et al., 2019. Migrating scarps as a significant driver for cometary surface evolution. GRL 46 (22), 12794–12804.

Britt, D.T., Boice, D.C., Buratti, B.J., Campins, H., Nelson, R.M., et al., 2004. The morphology and surface processes of comet 19/P Borrelly. Icarus 167, 45–53.

Brown, M.E., 2013. The density of mid-sized Kuiper Belt object 2002 UX25 and the formation of the dwarf planets. ApJ 778, L34 (5pp).

Choi, Y.-J., Cohen, M., Merk, R., Prialnik, D., 2002. Long-term evolution of objects in the Kuiper Belt zone – effects of insolation and radiogenic heating. Icarus 160 (2), 300–312.

Cotto-Figueroa, D., Statler, T.S., Richardson, D.C., Tanga, P., 2015. Coupled spin and shape evolution of small rubble-pile asteroids: self-limitation of the YORP effect. ApJ 803, 25 (18pp.).

Davidsson, B.J.R., Sierks, H., Güttler, C., Marzari, F., Pajola, M., et al., 2016. Ther primordial nucleus of comet 67P/Churyumov-Gerasimenko. A&A 592, A63 (30pp).

De Sanctis, M.C., Capria, M.T., Coradini, A., 2001. Thermal evolution and differentiation of Edgeworth-Kuiper Belt objects. AJ 121, 2792–2799.

De Sanctis, M.C., Capria, M.T., Coradini, A., Ammannito, E., 2007. Thermal evolution models of the 9P/Tempel 1 comet nucleus for interpreting the deep impact results. AJ 133, 1836–1846.

Desch, S.J., Cook, J.C., Doggett, T.C., Porter, S.B., 2009. Thermal evolution of Kuiper belt objects, with implications for cryovolcanism. Icarus 202, 694–714.

Drury, M.J., 1987. Thermal diffusivity of some crystalline rocks. Geothermics 16 (2), 105–115.

Farnham, T.L., Cochran, A.L., 2002. A McDonald observatory study of comet 19P/Borrelly: placing the deep space 1 observations into a broader context. Icarus 160, 398–418.

Grundy, W.M., Benecchi, S.D., Raninowitz, D.L., Porter, S.B., Wasserman, L.H., et al., 2012. Mutual events in the cold classical transnepunian binary system Sila and Nunam. Icarus 220, 74–83.

Grundy, W.M., Bird, M.K., Britt, D.T., Cook, J.C., Cruikshank, D.P., et al., 2020. Color, composition, and thermal environment of Kuiper Belt object (486958) Arrokoth. Science aay3705. https://doi.org/10.1126/science.aay3705 (12 pp.).

Guilbert-Lepoutre, A., Lasue, J., Federico, C., Coradini, A., Orosei, R., Rosenberg, E.D., 2011. New 3D thermal evolution model for icy bodies application to trans-Neptunian objects. A&A 529, A71 (11 pp.). https://doi.org/10.1051/0004-6361/201014194.

Guilbert-Lepoutre, A., Rosenberg, E.D., Prialnik, D., Besse, S., 2016. Modelling the evolution of a comet subsurface: implications for 67P/Churyumov-Gerasimenko. MNRAS 462, S146–S155. https://doi.org/10.1093/mnras/stw2371.

Gundlach, B., Blum, J., 2012. Outgassing of icy bodies in the solar system – II: heat transport in dry, porous surface dust layers. Icarus 219, 618–629.

Hirabayashi, M., Scheeres, D.J., Chesley, S.R., Marchi, S., McMahon, J.W., et al., 2016. Fission and reconfiguration of bilobate comets as revealed by 67P/Churyumov-Gerasimenko. Nature 534, 352–355.

Hirabayashi, M., Trowbridge, A.J., Bodewits, D., 2020. The mysterious location of Maryland on 2014 MU69 and the reconfiguration of its Bilobate shape. ApJL 89, L12 (6pp).

Hofgartner, J.D., Burati, B.J., Benecchi, S.D., Beyer, R.A., Cheng, A., et al., 2020. Photometry of Kuiper belt object (486958) Arrokoth from new horizons LORRI. Icarus. https://doi.org/10.1016/j.icarus.2020.113723 (In press. 2 March, 2020).

Hu, X., Shi, X., Sierks, H., Fulle, M., Blum, J., et al., 2017. Seasonal erosion and restoration of the dust cover on comet 67P/Churyumov-Gerasimenko as observed by OSIRIS onboard Rosetta. A&A 604, A114 (31 pp.).

Lai, I.L., Ip, W.H., Su, C.C., Wu, J.S., Lee, J.C., et al., 2016. Gas outflow and dust transport of comet 67P/Churyumov-Gerasimenko. MNRAS 462, S533–S546.

Keller, H.U., Mottola, S., Hviid, S.F., Agarwal, J., Kührt, E., et al., 2017. Seasonal mass transfer on the nucleus of comet 67P/Churyumov-Gerasimenko. MNRAS 469, S357–S371.

Kokotanekova, R., Snodgrass, C., Lacerda, P., Green, S.F., Lowry, S.C., Fernández, Y.R., et al., 2017. Rotation of cometary nuclei: new light curves and an update of the ensemble properties of Jupiter-family comets. MNRAS 471 (3), 2974–3007.

Kossacki, K.J., Jasiak, A., 2019. The evolution of gently sloping mantled deposits on comet 67P/Churyumov-Gerasimenko. Icarus 319, 381–391. https://doi.org/10.1016/j.icarus.2018.09.035.

Krijt, S., Schwarz, K.R., Bergin, E.A., Ciesla, F.J., 2018. Transport of CO in protoplanetary disks: consequences of pebble formation, settling, and radial drift. ApJ 864 (78). https://doi.org/10.3847/1538-4357/aad69b (18 pp.).

Langmuir, I., 1913. The vapor pressure of metallic tungsten. Phys. Rev. II 5, 329–342.

Lisse, C.M., Young, L.A., Cruikshank, D.P., Sandford, S.A., Stern, S.A., et al., 2020. On the stability of KBO 2014 MU_{69}'s Ices. Icarus (This issue).

Lyra, W., Youdin, A.N., Johansen, A., Umurhan, O.M., 2020. Evolution of MU69 from a binary planetesimal into contact by Kozai-Lidov oscillations and nebular drag. Icarus. https://doi.org/10.1016/j.icarus.2020.113831 (In revision).

Marshall, D., Groussin, O., Vincent, J.-B., Brouet, Y., Kappel, D., et al., 2018. Thermal inertia and roughness of the nucleus of comet 67P/Churyumov-Gerasimenko from MIRO and VIRTIS observations. A&A 616, A122 (13 pp.). https://doi.org/10.1051/0004-6361/201833104.

McKinnon, W.B., Richardson, D.C., Marohnic, J.C., Keane, J.T., Grundy, W.M., et al., 2020. The solar nebula origin of (486958) Arrokoth, a primordial contact binary in the Kuiper Belt. Science. https://doi.org/10.1126/science/aay6620.

Merk, R., Prialnik, D., 2003. Early thermal and structural evolution of small bodies in the trans-Neptunian zone. Earth Moon Planet. 92, 359–374.

Mueller, B.E.A., Samarasinha, N.H., 2018. Further investigation of changes in cometary rotation. AJ 156, 107 (7pp.).

Pätzold, M., Andert, T., Hahn, M., Asmar, S.W., Barriot, J.P., et al., 2016. A homogeneous nucleus for comet 67P/Churyumov-Gerasimenko from its gravity field. Nature 530, 63–65.

Preusker, F., Scholten, F., Matz, K.-D., Roatsch, T., Hviid, S.F., et al., 2017. The global meter-level shape model of comet 67P/Churyumov-Gerasimenko. A&A 607, L1 (5 pp.). https://doi.org/10.1051/0004-6361/201731798.

Prialnik, D., Podolak, M., 1995. Radioactive heating of porous comet nuclei. Icarus 117, 420–430.

Prialnik, D., Benkhoff, J., Podolak, M., 2004. Modeling the structure and activity of comet nuclei. In: Comets II, pp. 359–387.

Prialnik, D., Sarid, G., Rosenberg, E.D., Merk, R., 2008. Thermal and chemical evolution of comet nuclei and Kuiper Belt objects. Space Sci. Rev. 138, 147–164.

Richardson, J.E., Bowling, T.J., 2014. Investigating the combined effect of shape, density, and rotation on small body surface slopes and erosion rates. Icarus 234, 53–65.

Richardson, J.E., Melosh, H.J., Lisse, C.M., Carcich, B., 2007. A ballistics analysis of the deep impact ejecta plume: determining comet Tempel 1's gravity, mass, and density. Icarus 190, 357–390.

Rosenberg, E.D., Prialnik, D., 2010. The effect of internal inhomogeneity on the activity of comet nuclei – application to comet 67P/Churyumov-Gerasimenko. Icarus 209 (2), 753–765.

Rozitis, B., Green, S.F., 2013. The influence of global self-heating on the Yarkovsky and YORP effects. Mon. Not. R. Astron. Soc. 433 (1), 603–621.

Sagan, C., Mullen, G., 1972. Earth and Mars: evolution of atmospheres and surface temperatures. Science 177, 52–56.

Samarasinha, N.H., Mueller, B.E.A., 2013. Relating changes in cometary rotation to activity: current status and applications to comet C/2012 S1 (ISON). ApJ Lett. 775 (L10), 6pp.

Sarid, G., Prialnik, D., 2009. From KBOs to centaurs: the thermal connection. Meteorit. Planet. Sci. 44, 1905–1916.

Scheeres, D.J., 2007. The dynamical evolution of uniformly rotating asteroids subject to YORP. Icarus 188, 430–450.

Spencer, J.R., Stern, S.A., Moore, J.M., Weaver, H.A., Singer, K.N., et al., 2020. The geology and geophysics of Kuiper Belt object (486958) Arrokoth. Science aay3999. https://doi.org/10.1126/science.aay3999 (12 pp.).

Statler, T.S., 2009. Extreme sensitivity of the YORP effect to small-scale topography. Icarus 202, 502–513.

Steckloff, J.K., Jacobson, S.A., 2016. The formation of striae within cometary dust tails by a sublimation-driven YORP-like effect. Icarus 264, 160–171.

Steckloff, J.K., Samarasinha, N.H., 2018. The sublimative torques of Jupiter family comets and mass wasting events on their nuclei. Icarus 312, 172–180.

Steckloff, J.K., Johnson, B.C., Bowling, T., Melosh, H.J., Minton, D., Lisse, C.M., Battams, K., 2015. Dynamic sublimation pressure and the catastrophic breakup of comet ISON. Icarus 258, 430–437.

Stern, S.A., Weaver, H.A., Spencer, J.R., Olkin, C.B., Gladstone, G.R., Grundy, W.M., et al., 2019. Initial results from the new horizons exploration of 2014 MU_{69}, a small Kuiper Belt objects. Science 364, eaaw9771 (12 pp.).

Tang, Y., Birch, S.P.D., Hayes, A.G., Kirk, R., Kutsop, N., 2019. Generation of photoclinometric DTMs for application to transient changes on the surface of comet 67P/Churyumov-Gerasimenko. A&A 630, A10 (8 pp.). https://doi.org/10.1051/0004-6361/201834127.

Thomas, P., et al., 2013a. The nucleus of comet 9P/Tempel 1: shape and geology from two flybys. Icarus 222, 453–466.

Thomas, P.C., et al., 2013b. Shape, density, and geology of the nucleus of comet 103P/Hartley 2. Icarus 222, 550–558.

Vilenius, E., Kiss, C., Müller, T., Mommert, M., Santos-Sanz, P., et al., 2014. "TNOs are cool": a survey of the trans-Neptunian region. X. Analysis of classical Kuiper belt objects from Herschel and Spitzer observations. A&A 564, A35 (18 pp.).

Vilenius, W., Kiss, C., Mommert, M., Müller, T., Santos-Sanz, P., et al., 2012. "TNOs are cool": a survey of the trans-Neptunian region VI. Herschel/PACS observations and thermal modeling of 19 classical Kuiper belt objects. A&A 541, A94 (17 pp).

Williams, J.P., Cieza, L.A., 2011. Protoplanetary disks and their evolution. Annu. Rev. Astron. Astrophys. 49, 67–117.